

# Effect of grain size on R-curve behaviour of alumina ceramics

H. Tomaszewski \*, M. Boniecki, H. Weglarz

*Institute of Electronic Materials Technology, Wolczynska 133, 01-919 Warsaw, Poland*

Received 26 February 2000; received in revised form 15 April 2000; accepted 29 April 2000

---

## Abstract

Alumina samples with average grain sizes ranging from 2.6 to 67.4  $\mu\text{m}$  were prepared by sintering at 1500–1900°C for 2–20 h in high vacuum. Crystallographic and thermal expansion mismatch between adjacent grains during cooling involved residual stresses in these ceramics. The effect of these stresses on fracture behaviour of alumina ceramics was investigated by testing controlled crack growth during three point bending of single-edge-notched samples. After initiation, the crack grew slowly by repeated loading and unloading. The crack length  $c$ , was measured and registered in situ by means of a CCD camera coupled to an appropriate microscope, which was fitted to the test equipment by a system of elevator stages driven by stepping motors. The force  $P$ , necessary to produce an increasing crack length was computer controlled. The stress intensity factor  $K_I$ , was calculated from values of the crack length  $c$ , and force  $P$ . The data of  $K_I=f(c)$  obtained in the range of crack lengths studied were fitted by a linear function  $y=ax+b$ . As a result, the slope was used as a parameter describing R-curve behaviour of ceramics. The tests showed that R-curve behaviour of alumina ceramics strongly increases with the increase of  $\text{Al}_2\text{O}_3$  grain size. This phenomenon was explained by analysis of microstructures and residual stresses found in ceramics by piezospectroscopic measurements. In several samples the crack growth tests were performed without unloading. The time dependent displacement  $d$  of the sample was measured and recorded together with values of force  $P$ . The stress intensity factor  $K_I$ , maximal stress intensity factor  $K_{I_{\text{max}}}$ , resistance to crack initiation  $K_{I_i}$ , and work-of-fracture  $\gamma_F$ , were inferred from measured data. © 2000 Elsevier Science Ltd. All rights reserved.

*Keywords:*  $\text{Al}_2\text{O}_3$ ; Crack growth; Grain size; Mechanical properties; R-curve

---

## 1. Introduction

In recent years, much attention has been drawn to the phenomenon of a systematically increasing fracture resistance with crack extension in noncubic and non-transforming ceramics. To explain this phenomenon, a grain-bridging model of crack resistance or toughness (R-curve, or T-curve) properties of ceramics was developed in 1989 by Bennison et al.<sup>1</sup> By taking into account the internal residual stresses in the constitutive stress-separation relation for pullout of interlocking grains from an embedding matrix, the model manifests its importance in the treatise of fracture mechanics. These internal stresses are expected to play a controlling role in the toughness properties since they determine the scale of frictional tractions at the sliding grain–matrix interface. The importance of residual stresses in determining R-curve behaviour was clearly demonstrated in

the alumina-anorthite system.<sup>2</sup> Moreover, it is postulated that the extent of toughening also depends upon such factors as the size and shape of the bridging grains and the spacing between the bridges. The interrelationships between strength, crack-resistance characteristics and grain size for alumina ceramics in the size range 2–80  $\mu\text{m}$  were investigated by Chantikul et al.<sup>3</sup> T-curves as a function of grain size were obtained in this case by deconvolution of strength-indentation data. As a result, it was found that the toughness curves increase markedly, especially for the larger grain size structures.

The aim of this work was to determine the role of grain size in the R-curve behaviour of alumina ceramics by in situ measurement of controlled crack growth. The results obtained were related to residual stresses present in the studied ceramics.

## 2. Experimental methods

The starting material was alumina ceramic powder having the following chemical composition:  $\text{Al}_2\text{O}_3$ -99.55 wt.%,  $\text{MgO}$ -0.20 wt.%,  $\text{Y}_2\text{O}_3$ -0.25 wt.%. Two alumina

---

\* Corresponding author. Tel.: +48-22-8353041 ext. 472; fax: +48-22-8349003.

E-mail addresses: tomasz\_h@sp.itme.edu.pl, or itme@sp.itmt.edu.pl (H. Tomaszewski).

powders were used. The first one was alumina (CEMAT, Poland) made from ammonia alum (4N concentration) with an average grain size below  $0.5 \mu\text{m}$ . The second alumina powder was AKP-53 (Sumitomo, Japan) with an average particle size of  $0.3 \mu\text{m}$ . The two additives were analytically pure. The self-composed mixtures were homogenised in distilled water during 48 h in a ball mill and afterwards dried until they reached equilibrium humidity. Finally they were cold pressed under 120 MPa and sintered at  $1500\text{--}1900^\circ\text{C}$  for 1–20 h in a vacuum furnace. The sintered specimens were cut and ground to the dimensions of  $1.5 \times 6 \times 45 \text{ mm}$  and one surface was polished. In the central part of the samples, a sharp notch was prepared.<sup>4</sup> Then the polished surface of the samples was covered with a 150 nm thick Al layer to improve the visibility of the crack path during the test of controlled crack growth.

For the measurement of Young's modulus the beams were trimmed to the height of 1 mm and then compliance of the samples was recorded during loading tests using an universal testing machine (Model 1446, Zwick) with 0.1 mm/min loading speed and 40 mm bearing distance. The values of Young's modulus were calculated using the relation given by Fett and Munz.<sup>5</sup>

The tests of controlled crack growth were performed in three-point bending with 1  $\mu\text{m}/\text{min}$  loading speed and 40 mm bearing distance using the same testing machine. The crack was initiated and slowly grew up by repeated loading and unloading. The crack length  $c$ , was measured in situ using a CCD camera coupled to an appropriate microscope, which was fitted to the test equipment by a system of elevator stages driven by stepping motors. This enabled the precise movement of the microscope objective in  $x$ - $y$ - $z$  directions for adjustment, focussing and tracking on the beam side and bottom surface where the crack propagated. A measuring and registration system (framegrabber) was coupled with the load and strain system of the testing machine. Both systems were computer controlled. The optical and electronic magnifications were about  $250\times$ . Typical path of cracks propagated in alumina ceramics are shown in Fig. 1. The stress intensity factor  $K_I$ , was calculated from the crack length  $c$ , and force  $P$ .<sup>5</sup> The data of  $K_I=f(c)$  obtained in the range of crack length studied were fitted by a linear function  $y=ax+b$  and the slope  $a$ , was used as a parameter describing R-curve behaviour. All experiments were done at room temperature in normal air environments.

In several samples the crack growth tests were done without unloading. The time dependent displacement  $d$ , of the sample was measured and recorded together with values of force  $P$ . By the procedure described earlier<sup>6</sup> the maximal stress intensity factor  $K_{I\text{max}}$ , and the resistance to crack initiation  $K_{Ii}$ , were calculated. Given that the area under the recorded load-deflection curve of the

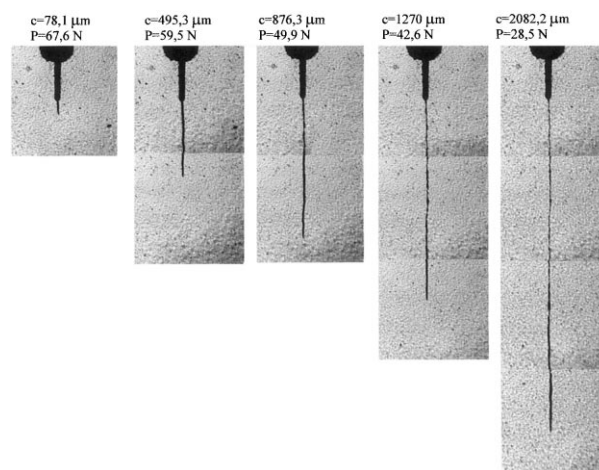


Fig. 1. An example of succeeding steps of a crack propagation in an alumina ceramics as stored on a computer disc. On top of the images the applied force  $P$ , at which a crack of length  $c$  was generated, is given.

specimen is the sum of the work used for the creation of two new surfaces and the elastic strain energy of the system and sample studied, the work-of-fracture  $\gamma_F$  was determined.<sup>6</sup>

Residual stresses within the alumina were measured using the piezospectroscopic technique described elsewhere.<sup>4,6</sup> An optical microscope was used to both excite the fluorescence and to collect and analyse the resulting fluorescence spectrum using an attached spectrometer (DILOR X4800). The 514.5 nm line of an argon ion laser was used to excite the fluorescence. The fluorescence signals were collected from a region of about  $50 \mu\text{m}$  diameter in size. The intensity of the  $R_1$  and  $R_2$  fluorescence lines was scanned by integrating over 0.5 s intervals at a spacing of 0.2 wavenumbers with the intensity being recorded under computer control. The collected data were subsequently analysed with curve-fitting algorithms (double Lorenz function). The line position was identified by simultaneously fitting the  $R_1$  and  $R_2$  peaks using the NiceFit software package. All measurements were performed at room temperature. The peak shift due to eventual temperature fluctuations was corrected using the ruby calibration. The instrumental shift was also corrected by simultaneously monitoring a characteristic Neon line at  $14564 \text{ cm}^{-1}$ . The average residual stress in the alumina matrix was calculated from the measured frequency shifts according to a relation of linear proportionality by means of the average piezospectroscopic coefficients given by He and Clarke.<sup>7</sup>

Microstructure observations of the ceramics were performed on polished and thermally etched surfaces using a OPTON DSM 950 SEM microscope. Grain size distribution measurements have also been made (see Fig. 2).

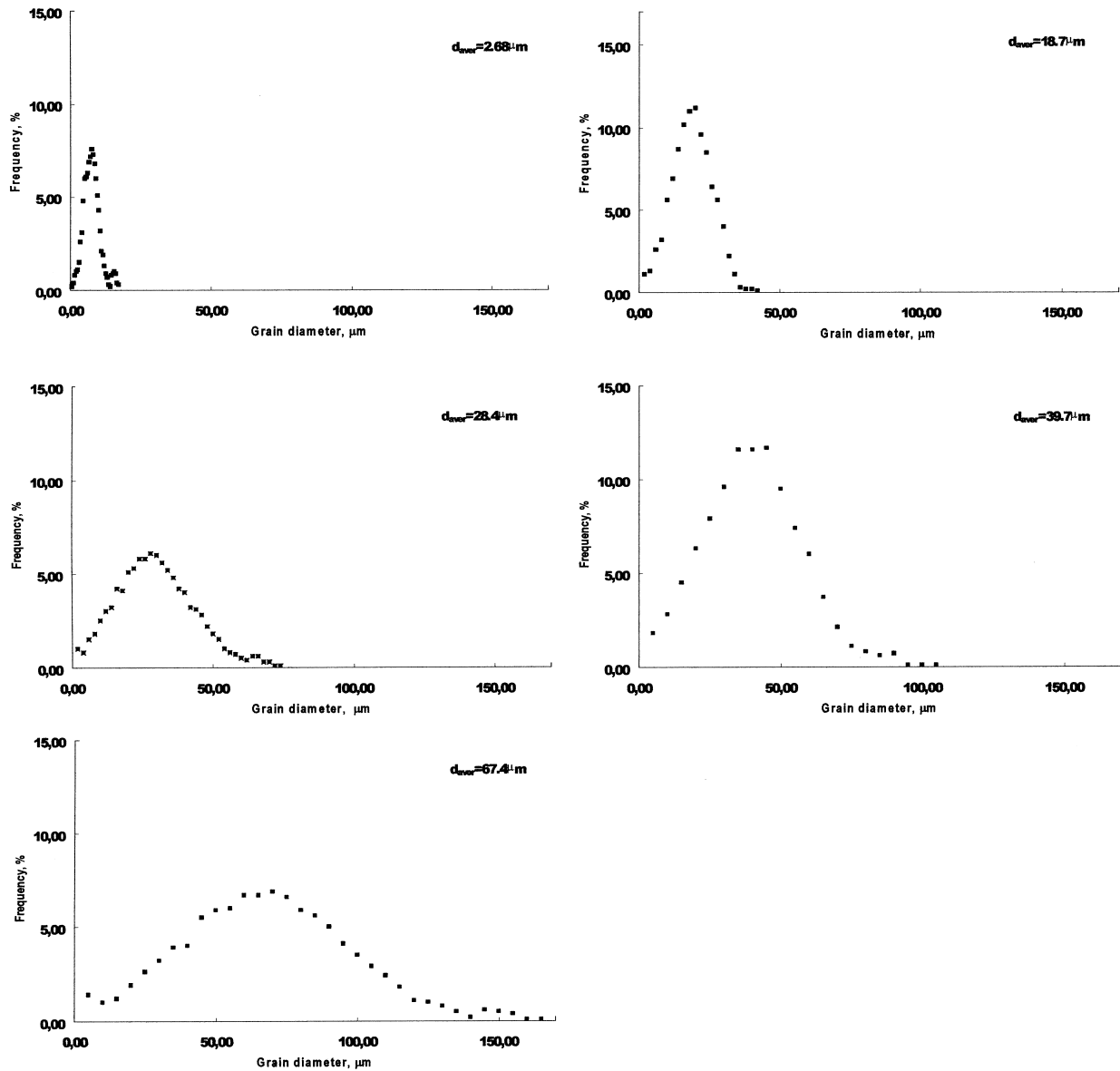


Fig. 2.  $\text{Al}_2\text{O}_3$  grain size distribution in alumina ceramics.

### 3. Results and discussion

As mentioned by Bennison et al.,<sup>1</sup> due to anisotropy in crystallographic and thermal properties of alumina, some grains in the alumina matrix are subjected to compression and play the role of “bridges”. The remaining grains, subject to tension, are considered as making up the constitutive “matrix”. The bridging grains, wedged in the microstructure by this internal compressive stress, lead to an increase in fracture toughness as the crack grows.

Such bridging grains, surrounded by a propagating crack were observed in samples studied during controlled crack growth tests (see Fig. 3). A dependence of the amount of bridging grains on  $\text{Al}_2\text{O}_3$  grain size was also found. From Table 1 it can be seen that the part

(%) of a whole path length of the crack propagating through an alumina ceramic and which surrounds a bridging grain, increases with increasing size of the alumina grains.

Generally the intergranular fracture mode was observed in alumina samples independent of grain size. However, for larger grain size microstructures some branching of the crack was also found (see Table 1).

As was stated by Bennison et al.<sup>1</sup> the bridging grains are expected to influence the stress intensity factor  $K_I$  as the crack grows. The data of  $K_{Ic} = f(c)$  obtained in the range of crack lengths studied were fitted by a linear equation  $y = ax + b$  and the slope  $a$  was used as a factor describing the R-curve behaviour of ceramics. Values of parameters  $a$  and  $b$  in function of grain size are listed in Table 2. The slope parameter  $a$  strongly increases from

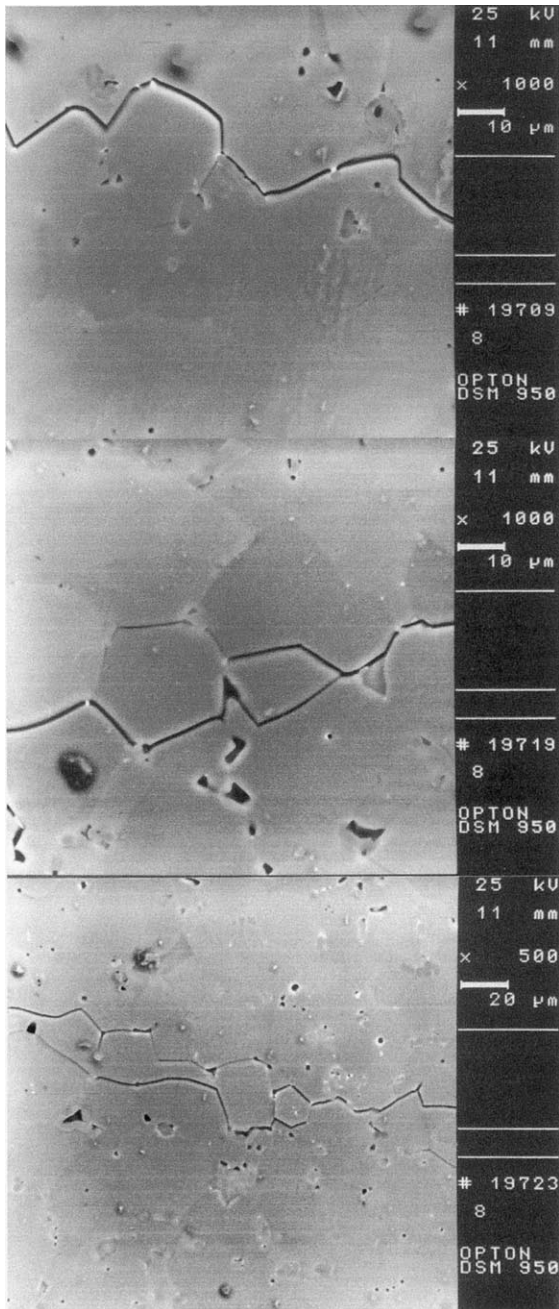


Fig. 3. Single and a group of  $\text{Al}_2\text{O}_3$  grains acting as bridging grains, observed in alumina ceramics.

0.44 to 1.89 as the  $\text{Al}_2\text{O}_3$  grain size increases from 2.6 to 67.4  $\mu\text{m}$  (Table 2 and Fig. 4). Decrease of R-curve behaviour of alumina with decreasing grain size allows the assumption that a grain size should exist where the slope  $a$  equals zero.

Decrease of  $\text{Al}_2\text{O}_3$  grain size affects not only the amount of bridging grains but also the mean value of residual stresses generated by thermal expansion anisotropy of alumina (see Table 3). Although the sum of stresses over the material must be zero, variations in stress from one grain to another cause both line shift and a broadening. As a result it is possible to calculate first the average values of the line shift  $\Delta v$ , and then the mean values of residual stresses present in the ceramics. Table 3 shows that the mean stress measured by piezospectroscopy strongly decreases with  $\text{Al}_2\text{O}_3$  grain size. It means that a decrease of frictional forces acts during grain pullout of the embedding matrix, resulting in a decrease of R-curve behaviour (see values of slope  $a$  in Table 2) of alumina ceramics.

For some samples of ceramics the tests of crack growth were performed without removing the load. The values of maximal stress intensity factor  $K_{I\text{max}}$ , resistance to crack initiation  $K_{Ii}$ , and work-of-fracture  $\gamma_F$  are listed in Table 4. As can be seen,  $K_{I\text{max}}$  of alumina increases significantly with increasing  $\text{Al}_2\text{O}_3$  grain size, while, however, only a small decrease of resistance to crack initiation ( $K_{Ii}$ ) is observed. Increasing values of work-of-fracture with increasing grain size can be related to the elongation of the crack path observed, due to grain bridging and crack deflection (see Table 1).

#### 4. Summary

The aim of this work was to determine the effect of microstructure and residual stresses on R-curve properties of alumina ceramics. To realise this, alumina samples with grains in the size range 2.6–67  $\mu\text{m}$  were prepared. Residual stresses, generated by thermal expansion anisotropy of  $\text{Al}_2\text{O}_3$  and dependent on grain size, were found in the ceramics. Tests of controlled crack growth for all samples were performed. Data of  $K_I=f(c)$  obtained in the range of crack length studied

Table 1  
Crack path elements measured in alumina ceramics as a function of  $\text{Al}_2\text{O}_3$  grain size

$\text{Al}_2\text{O}_3$ grain size, $\mu\text{m}$	2.6±0.8	18.6±8.9	28.4±13.7	39.7±17.2	67.4±29.4
Part of a crack path length surrounding bridging grains, %	3.4	10.7	24.8	40.3	64.9
Branching part of a crack path length, %	0	0	0	2.1	9.8
Relative elongation of a crack path length due to grain bridging and grain deflection, $l/l_0$	1.24	1.27	1.60	1.80	2.29

Table 2  
Linear coefficients  $a$  and  $b$  (from equation  $y = ax + b$ ) as a function of  $\text{Al}_2\text{O}_3$  grain size

$\text{Al}_2\text{O}_3$ grain size, $\mu\text{m}$	2.6±0.8	18.6±8.9	28.4±13.7	39.7±17.2	67.4±29.4
$a$	0.44±0.19	0.66±0.03	1.02±0.09	1.60±0.03	1.89±0.14
$b$	3.17±0.45	3.17±0.08	1.94±0.09	0.80±0.28	0.13±0.27

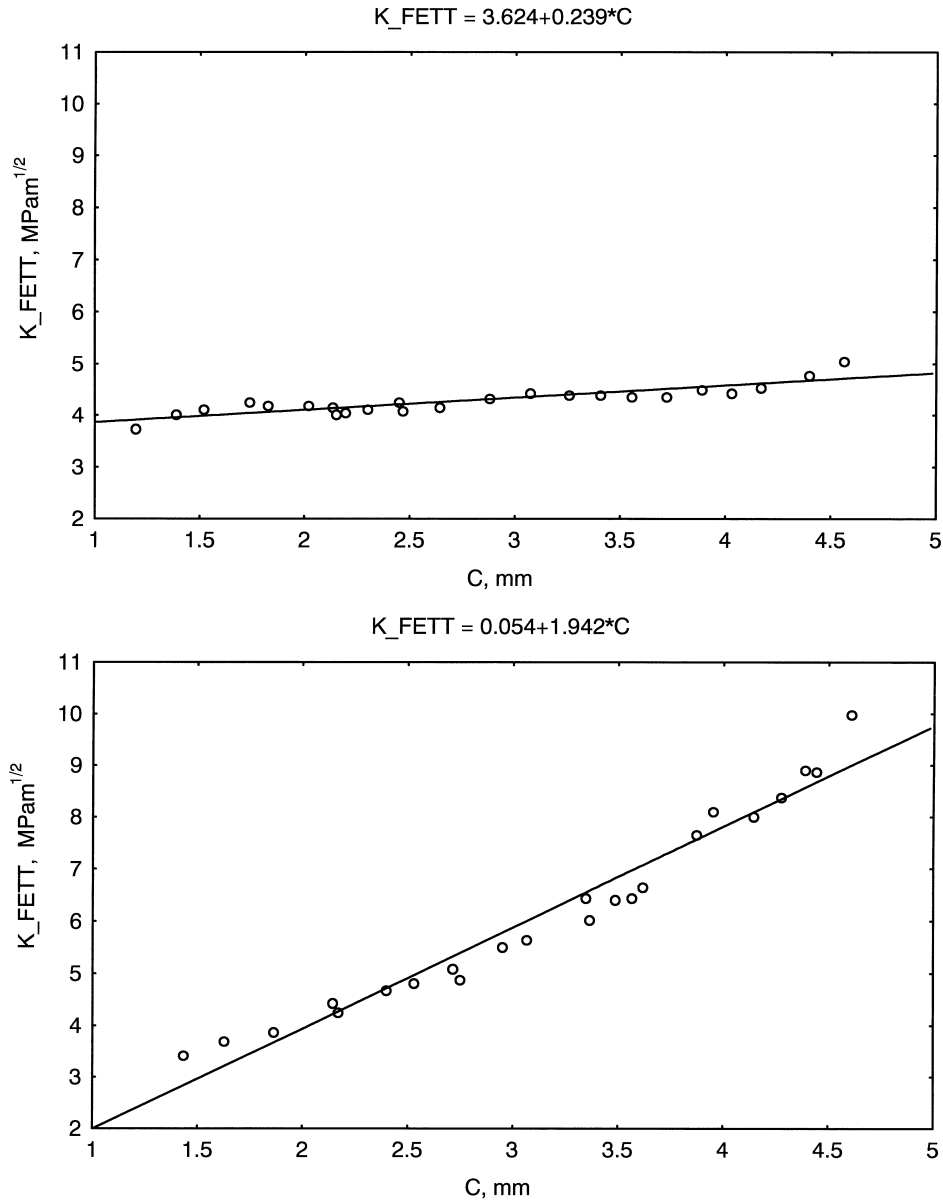


Fig. 4. Dependence of  $K_I$  on the crack length  $c$  for alumina ceramics with 2.6  $\mu\text{m}$  (top) and 67.4  $\mu\text{m}$   $\text{Al}_2\text{O}_3$  grain size (bottom).

Table 3  
Mean values of residual stresses measured in alumina ceramics as a function of  $\text{Al}_2\text{O}_3$  grain size

$\text{Al}_2\text{O}_3$ grain size, $\mu\text{m}$	2.6±0.8	18.6±8.9	28.4±13.7	39.7±17.2	67.4±29.4
Mean value of residual stress, MPa	63.1±11.8	78.9±15.8	118.4±27.6	110.5±31.5	126.3±43.4

Table 4

Maximal stress intensity factor  $K_{I\max}$ , resistance to crack initiation  $K_{Ii}$ , and work-of-fracture,  $\gamma_F$  for alumina ceramics as a function of  $\text{Al}_2\text{O}_3$  grain size

$\text{Al}_2\text{O}_3$ grain size, $\mu\text{m}$	$K_{I\max}$ , $\text{MPam}^{1/2}$	$K_{Ii}$ , $\text{MPam}^{1/2}$	$\gamma_F$ , $\text{J/m}^2$
$2.6 \pm 0.8$	$4.48 \pm 0.39$	$3.27 \pm 0.33$	$26.92 \pm 1.80$
$18.6 \pm 8.9$	$5.02 \pm 0.38$	$2.99 \pm 0.15$	$29.55 \pm 2.56$
$28.4 \pm 13.7$	$5.36 \pm 0.39$	$2.94 \pm 0.13$	$31.37 \pm 2.18$
$39.7 \pm 17.2$	$6.05 \pm 0.34$	$2.69 \pm 0.09$	$31.58 \pm 3.67$
$67.4 \pm 29.4$	$6.31 \pm 0.13$	$2.72 \pm 0.18$	$36.44 \pm 5.45$

were approximated by a linear equation  $y = ax + b$ . As a result the slope parameter  $a$  was used as a factor describing the R-curve behaviour of ceramics. A decrease in slope  $a$  with a decrease in  $\text{Al}_2\text{O}_3$  grain size was found. Observed changes were related to the amount of bridging grains on the path of the propagating crack and the residual stresses present in the ceramics. For some samples of ceramics the tests of crack growth were performed without removing the load. The values of maximal stress intensity factor  $K_{I\max}$ , resistance to crack initiation  $K_{Ii}$ , and work-of-fracture  $\gamma_F$ , were calculated. An increase of  $K_{I\max}$  and  $\gamma_F$  with increasing  $\text{Al}_2\text{O}_3$  grain size was observed.

## References

1. Bennison, S. J. and Lawn, B. R., Role of interfacial grain-bridging sliding friction in the crack-resistance and strength properties of nontransforming ceramics. *Acta Metall.*, 1989, **37**(10), 2659–2671.
2. Padture, N. T. and Chan, H. M., Improved flaw tolerance in alumina containing 1 vol.% anorthite via crystallization of the intergranular glass. *J. Am. Ceram. Soc.*, 1982, **75**(7), 1870–1875.
3. Chantikul, P., Bennison, S. J. and Lawn, B. R., Role of grain size in the strength and R-curve properties of alumina. *J. Am. Ceram. Soc.*, 1990, **73**(8), 2419–2427.
4. Tomaszewski, H., Strzeszewski, J. and Gebicki, W., The role of residual stresses in layered composites of Y–ZrO<sub>2</sub> and Al<sub>2</sub>O<sub>3</sub>. *J. Eur. Ceram. Soc.*, 1999, **19**, 255–262.
5. Fett, T. and Munz, D., Subcritical crack growth of macrocracks in alumina with R-curve behaviour. *J. Am. Ceram. Soc.*, 1992, **75**(4), 958–963.
6. Tomaszewski, H., Weglarz, H., Boniecki, M. and Recko, M., Effect of barrier layer thickness and composition on fracture toughness of layered zirconia/alumina composites. *J. Mat. Sci.*, in press.
7. He, J. and Clarke, D. R., Determination of the piezo-spectroscopic coefficients for chromium-doped sapphire. *J. Am. Ceram. Soc.*, 1995, **78**(5), 1341–1353.